Heliyon 6 (2020) e03124

Contents lists available at ScienceDirect

Heliyon

journal homepage: www.cell.com/heliyon

Research article

Effects of PEGylated Fe–Fe_3O_4 core-shell nanoparticles on NIH3T3 and A549 cell lines

B.H. Domac [a,1], S. AlKhatib [b,1], O. Zirhli [a,c], N.G. Akdogan [d], Ş.C. Öçal Dirican [e], G. Bulut [f,**], O. Akdogan [a,*]

[a] Mechatronics Engineering, Faculty of Engineering and Natural Sciences, Bahçeşehir University, 34353, Istanbul, Turkey
[b] Bioengineering Program, Graduate School of Natural and Applied Sciences, Bahçeşehir University, 34353, Istanbul, Turkey
[c] Faculty of Engineering and Natural Sciences, Sabancı University, 34956, Istanbul, Turkey
[d] Faculty of Engineering, Piri Reis University, 34940, Istanbul, Turkey
[e] Biology Program, Graduate School of Natural and Applied Sciences, Ankara University, 06110, Ankara, Turkey
[f] Department of Molecular Biology and Genetics, Faculty of Engineering and Natural Sciences, Bahçeşehir University, 34353, Istanbul, Turkey

ARTICLE INFO

Keywords:
Drug delivery
Biophysics
Magnetism
Nanoparticle synthesis
Nanotechnology
Chemotherapy
Fe–Fe_3O_4 nanoparticles
Targeted drug delivery

ABSTRACT

Magnetic nanoparticles are key components in many fields of science and industry. Especially in cancer diagnosis and therapy, they are involved in targeted drug delivery and hyperthermia applications due to their ability to be controlled remotely. In this study, a PEG-coated Fe/Fe_3O_4 core-shell nanoparticle with an average size of 20 nm and 13 nm and high room temperature coercivity (350 Oe) has been successfully synthesized. These nanoparticles were further tested for their effect on cellular toxicity (IC50) and proliferation by WST assay. In addition, their potential as anti-cancer agents were assessed using scratch assay in NIH3T3 mouse embryonic fibroblast and A549 non-small cell lung cancer cell lines.

In previous reports, the IC50 values of the magnetite nanoparticles are reported at concentrations of 100 μg/ml and higher. In this study, IC50 value is observed to be at 1 μg/ml, which is significantly lower when compared to similar studies. In scratch assay, the Fe/Fe3O4 core-shell nanoparticle showed a higher inhibitory potential on cell motility in A549 lung cancer cells in comparison to the NIH3T3 cells mouse embryonic fibroblasts. This could be due to the accelerated release of free Fe ion from the Fe core, resulting in cell death. Consequently, data obtained from this study suggest that the synthesized nanoparticles can be a potential drug candidate with anti-cancer activity for chemotherapeutic treatment.

1. Introduction

Cancer is considered a major health problem around the world and many attempts have been made to minimize cancer incidence and mortality. Currently, several types of treatments are used for cancer therapy including surgery, radiation, chemotherapy, immunotherapy and targeted therapy, which focus on targeting specific genes and proteins that promote cancer growth and cancer cell survival [1].

Nanotechnology has recently arrived on the scene as a new field of science that opens enticing prospects of several applications, such as the treatment of various diseases including cancer [2]. Nanotechnology provides ways to enhance the efficacy of cancer therapies in targeting only malignant cells without damaging healthy cells [3]. One of the latest advances in nanotechnology is the development of numerous nanoparticle formulations that are engineered to be suitable for cancer research [4].

Nanoparticles (NP) have emerged as novel diagnostic and therapeutic tools for cancer due to their distinctive features in terms of size, shape, and surface characteristics. Organic nanoparticles, such as polymeric micelles, liposomes and dendrimers, and inorganic nanoparticles, such as magnetic NPs, gold NPs, and silica NPs have been used in a drug delivery system as drug carriers. According to the size and shape of nanoparticles, the delivered anti-cancer agents can target the tumor more specifically

* Corresponding author.
** Corresponding author.
E-mail addresses: gulay.bulut@bahcesehir.edu.tr (G. Bulut), ozan.akdogan@eng.bau.edu.tr (O. Akdogan).
[1] B.H.Domac and S.AlKhatib contributed equally.

https://doi.org/10.1016/j.heliyon.2019.e03124
Received 27 July 2019; Received in revised form 1 November 2019; Accepted 23 December 2019

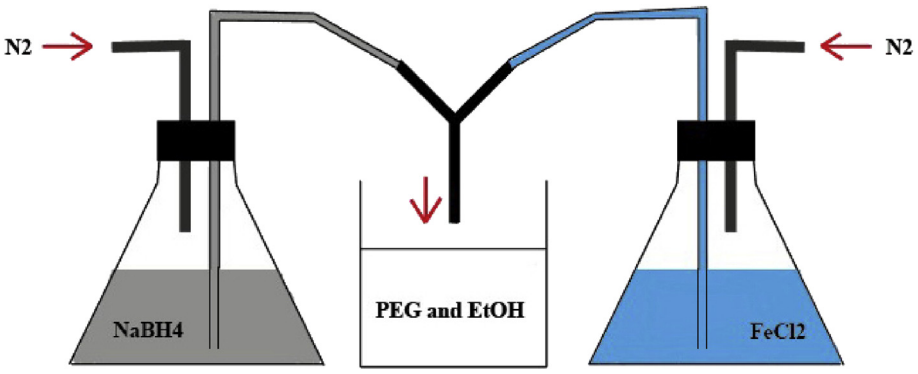

Figure 1. Schematics of nanoparticle synthesis setup.

with fewer side effects and a higher treatment efficacy relies on enhanced permeability and retention (EPR) [5, 6, 7, 8].

Fe_3O_4 (magnetite) particles are heavily used in cancer diagnosis and treatment due to their biocompatibility and biodegradability. Risk and benefit requirements of magnetite particles make them indispensable for MRI contrast enhancement, targeted drug delivery, and magnetic hyperthermia applications [9, 10]. The latter application requires high coercivity and magnetization.

The size of the nanoparticles directly affects the duration of the NP in the blood circulation. Particles bigger than 200 nm are easily cleared by the reticuloendothelial system, albeit smaller particles are easily cleared by the body through the kidneys. Furthermore, hydrophobicity and negatively charged particles are easily detected and cleared by the mononuclear phagocyte system (MPS). Thereupon, appropriate coating of the particles with synthetic polymers, surfactants, gold, silica, and peptides may be necessary [2].

Particles are generally coated with hydrophilic, uncharged and biocompatible coatings such as poly (ethylene glycol) (PEG) to prevent recognition by the MPS [11, 12, 13]. Thus, particles duration time in the blood circulation is extended. These nanoparticles reach a better performance for most of the aforementioned applications.

The effects of nanoparticles on living cells can vary depending on cell type, activity, type and size of the nanoparticle itself [14]. The aim of this study is to determine the effect of synthesized PEG-coated Fe/Fe_3O_4 nanoparticles on human non-small cell lung cancer A549 cells and mouse fibroblast NIH3T3 cells and evaluate their potential as anti-cancer agents. It is important to evaluate the toxicity of these nanoparticles by determining the half-maximal inhibitory concentration (IC50) on cultured cells. In parallel to this, cell proliferation assay, a widely applied method in nanotechnology to test the toxicity and effect of the nanoparticles on cell proliferation was performed [15]. Moreover, the possible effect of the nanoparticles on cell motility, which is a preliminary mechanism in

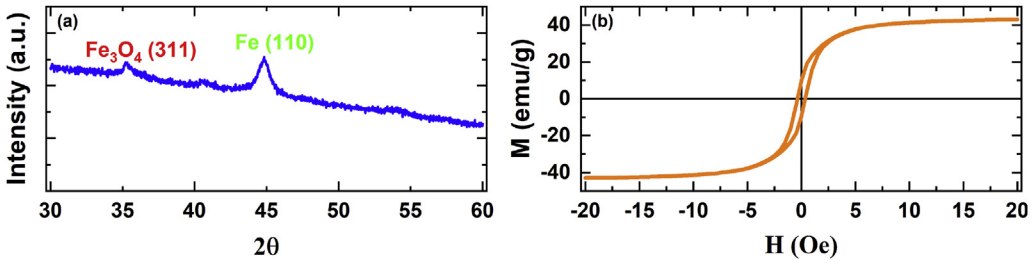

Figure 2. a. X-ray diffraction (Cu Ka1) and b. Vibrating Sample Magnetometer data of nanoparticles.

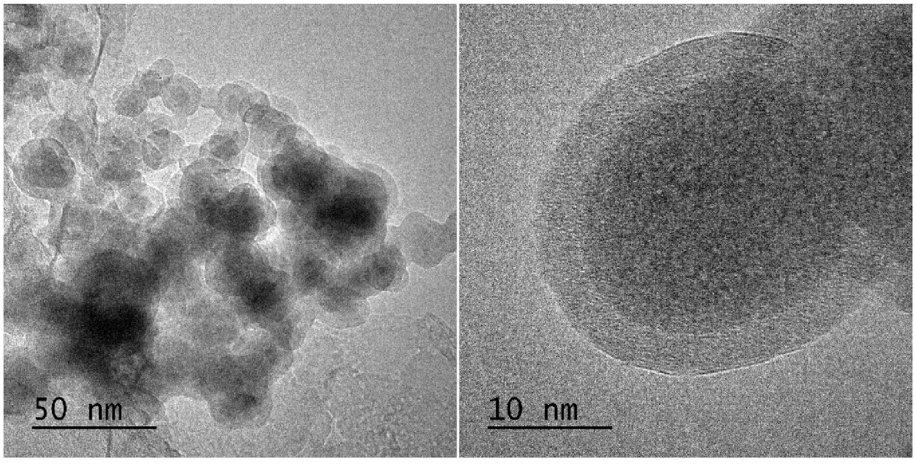

Figure 3. TEM bright-field image of NP1, showing the core-shell morphology.

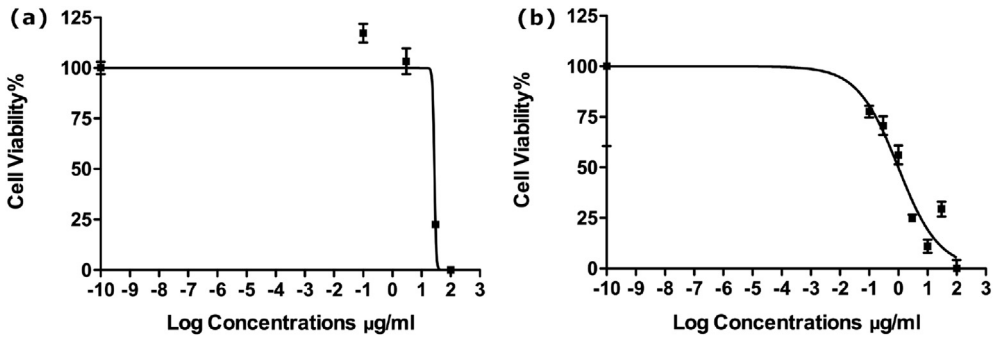

Figure 4. a. and b. Cell viability versus concentration plots of the NP1 at 0, 100 ng/ml, 300 ng/ml, 1 µg/ml, 3 µg/ml, 10 µg/ml, 30 µg/ml and 100 µg/ml concentrations on NIH3T3 and A549 cells, respectively.

cellular motility and the development of metastasis was analyzed through scratch assay [16].

2. Materials and methods

2.1. Nanoparticle synthesis

Nanoparticles were produced via salt reduction, using the Y junction flow tube technique. $FeCl_2$ and $NaBH_4$ were used as the salt and the reducer, respectively. In a typical synthesis route, $FeCl_2$ and $NaBH_4$ are dissolved separately in 50 ml DI water and degassed for 30 min under N_2 gas flow to get rid of free dissolved oxygen. The controllable mixture of these chemicals was assured by passing them through the Y junction flow tube (Figure 1). At the junction point, where the intermixing occurs, nanoparticles form and drop into the collection beaker. At this point, the particles get in touch with dissolved capping agents (surfactants, polymers, etc). In this study, PEG (10,000 MW) was used. PEG-coated Fe/Fe_3O_4 nanoparticles were cleaned from byproducts (NaCl, etc) of the chemical reaction for four times and the final product was stored in pure EtOH. Two different types of nanoparticles have been synthesized by changing the $NaBH_4/FeCl_2$ molar ratio; NP1: 1.67 and NP2: 0.85.

Morphological, structural and magnetic characterization of the nanoparticles was performed by JEOL JEM-ARM200CFEG UHR-TEM, Bruker D2 Phaser XRD, and EZ9 Microsense VSM, respectively.

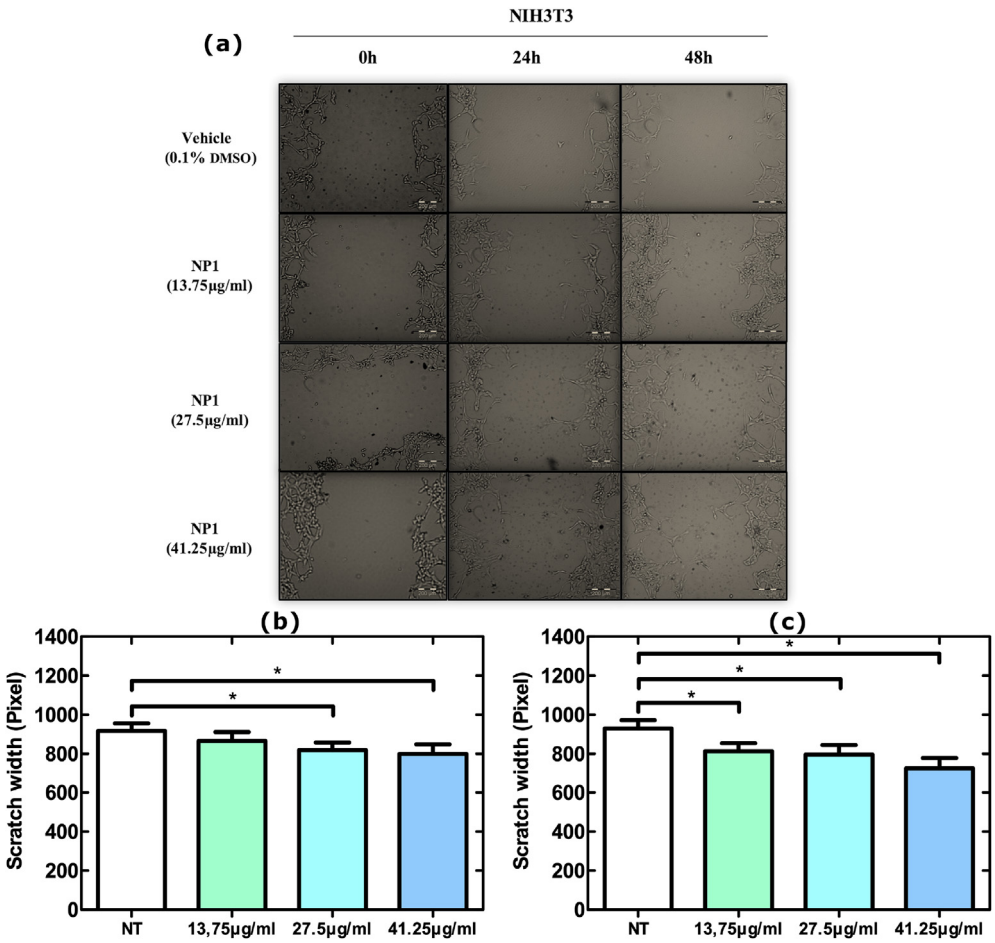

Figure 5. a. Microscopy images obtained in the wound healing experiment for three different NP1 concentrations (13.75 µg/ml, 27.5 µg/ml, and 41.25 µg/ml) in NIH3T3 cells. The measurement scale bar is 200µm. Scratch width pixel charts based on different concentrations of nanoparticles and treatment time (**b.** 24 h, **c.** 48 h) in NIH3T3 cells.

2.2. Cell culture

NIH3T3 mouse embryonic cells (CRL1658, ATCC) were grown in DMEM medium and A549 human non-small cell lung cancer cells (CCL185, ATCC) were grown in F12–K medium according to the manufacturer's protocol. All media were supplemented with 10% fetal bovine serum. Cells were maintained in 37 °C humidified atmosphere with 5% CO2.

2.3. Dilution of nanoparticles

Nanoparticles were dissolved in DMSO at 2 mg/ml stock concentration and stored at room temperature.

2.4. Cell proliferation assay

Cellular proliferation was analyzed using WST-1 Reagent (Roche). Cells were seeded at a density of 10,000 cells/well for NIH3T3 and 5,000 cells/well for A549 in a 96-well plate. The next day, both NIH3T3 and A549 cells were treated with nanoparticles at different concentrations in triplicates. After 48h, 10μl of WST-1 reagent was added onto the cells and cells were incubated for 30mins. Absorbance values were measured at 420nm using MultiScan GO Microplate spectrophotometer. The IC50 values were determined by GraphPad Prism Software.

2.5. Scratch assay

The effect of the nanoparticles on cellular motility was assessed using the scratch assay. Cells were plated at a density of 400,000–600,000 cells/well on a 6-well plate in order to form a confluent monolayer the following day. After 24h, a scratch was made on the cell surface using a sterile p-200 pipette tip. The scratched plate was washed with PBS to remove non-adherent cells. The cells were then treated with the nanoparticles at concentrations that were folds of the relevant IC50 values (NIH3T3 cells at 13.75 μg/ml, 27.5 μg/ml, and 41.25 μg/ml concentrations and A549 cells at 0.5 μg/ml, 1 μg/ml, and 2 μg/ml concentrations) for an additional 48h. Images were captured using an Olympus CRKX41 inverted microscope at 24h and 48h of incubation. The distance of migrated cells compared to the baseline distance was measured in pixels. The numerical data obtained was analyzed by GraphPad Prism software using "paired t-test ($p < 0.05$)".

3. Results and discussion

3.1. Structural, morphological and magnetic characterization of nanoparticles

XRD analysis of NP1 and NP2 shows that the nanoparticles are composed of α-Fe and Fe_3O_4 (Magnetite) phases (Figure 2a). The average particle size of NP1: 21nm and NP2: 13nm has been predicted from Scherer's Eq. ($D = 0.9\ \lambda/\beta\cos\theta$, λ: wavelength, β: FWHM, θ: diffraction angle) by using the full width at half maximum of the highest peak in XRD Data. Room temperature magnetic characterization reveals low magnetization and coercivity (Hc) of 350 Oe (Figure 2b). The high coercivity of these particles makes them suitable for hyperthermia applications due to high hysteresis loss [10, 11].

In order to study the morphology of the particles, TEM study was performed. The bright-field TEM image of the particles shows spherical

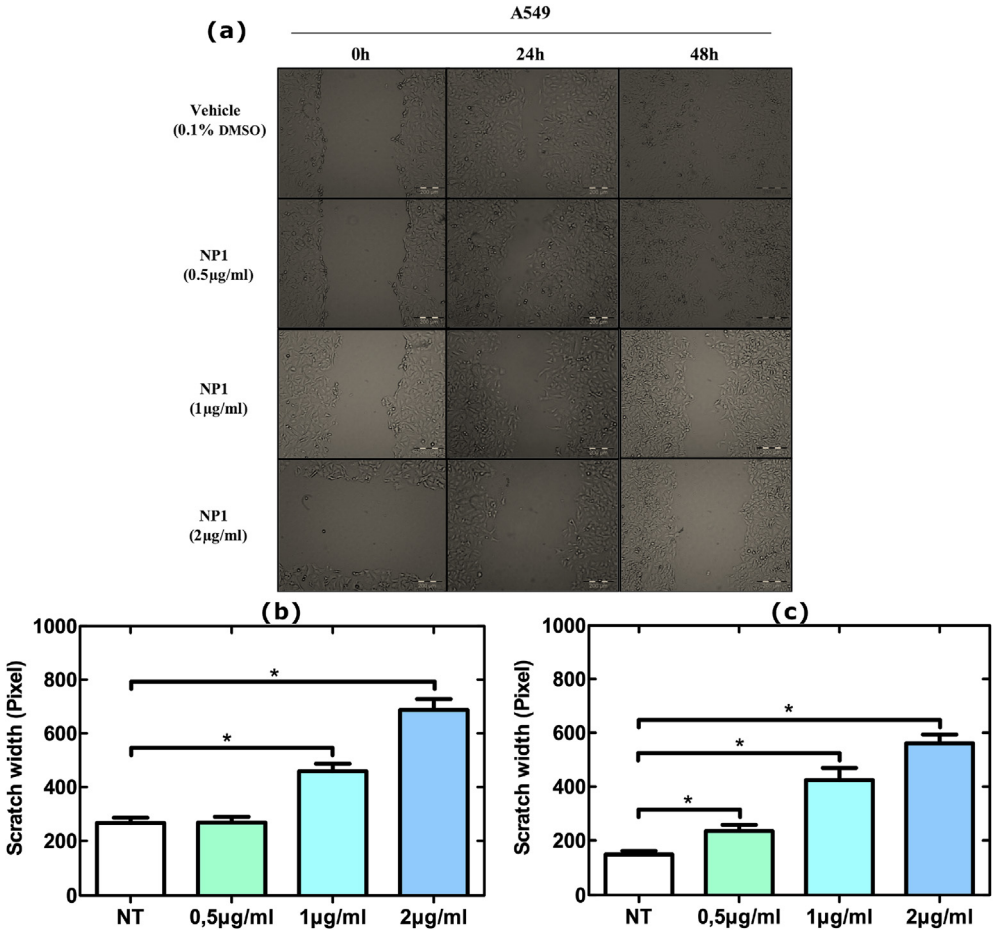

Figure 6. a. Microscopy images obtained in the scratch assay for three different NP1 concentrations (0.5 μg/ml, 1 μg/ml, and 2 μg/ml) in A549 cells. The measurement scale bar is 200μm. Scratch width pixel charts based on different concentrations and treatment time (**b.** 24 h, **c.** 48 h) of nanoparticles in A549 cells.

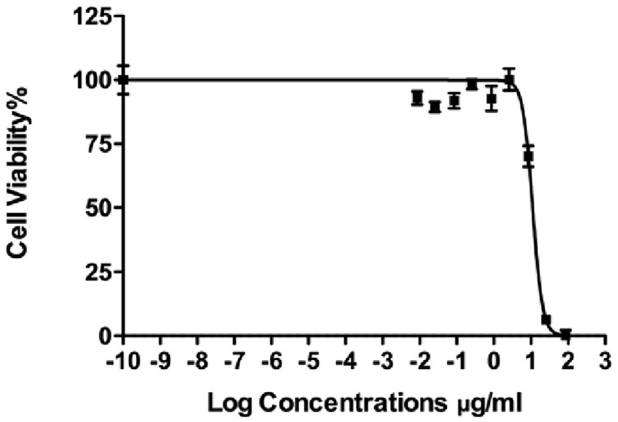

Figure 7. Cell viability versus concentration plots of the nanoparticles Paclitaxel at 0, 100 ng/ml, 300 ng/ml, 1 µg/ml, 3 µg/ml, 10 µg/ml, 30 µg/ml and100 µg/ml concentrations on A549 cells.

core-shell morphology, where the core is Fe with ≈20nm diameter, the shell is Fe_3O_4 with ≈3.5nm thickness (confirmed by energy dispersive x-ray spectroscopy) (Figure 3). Predicted values from the XRD data match with the size of the nanoparticles. Although PEG coating is not obvious in TEM bright-field images, PEG coating layer on the nanoparticles was realized due to the hydrophilic nature of the synthesized nanoparticles [2].

3.2. Cellular proliferation assay

Nanoparticles were dissolved in sterile DMSO and stored at room temperature. The stock concentration of the nanoparticles was prepared at 2 mg/ml. The final concentration of the DMSO administered on the cells was fixed at 0.1% due to the potential effect of this reagent on cell viability and proliferation.

NIH3T3 and A549 cells were treated with the NP1 at various concentrations (0–100 µg/ml). After incubation with the nanoparticles, 10µl of WST-1 reagent (Roche) was added onto the cells in order to check for the cell viability according to the manufacturer's protocol. The half-maximum inhibitory concentrations (IC50) of nanoparticles was found to be 27.5 µg/ml and 1 µg/ml in NIH3T3 and A549 cells, respectively. The cell viability versus log concentration plots are given in Figure 4.

3.3. Scratch assay

In order to test the potential of NP1 as an anti-cancer agent, scratch assay was performed on NIH3T3 and A549 cells. According to the data obtained on NIH3T3 cells, nanoparticles did not show a significant inhibitory role on cell motility when compared to the non-treated (negative control) cells both at 24 and 48 h of treatment (Figure 5). Cell death due to the toxic effect of NP1 on NIH3T3 cells was observed at 41.25 µg/ml concentration (two folds of the IC50 value) and 48h of treatment. On the contrary, nanoparticles had a significant inhibitory effect on the motility of A549 lung cancer cells when compared to the non-treated cells at 24 and 48 h of treatment (Figure 6).

4. Discussion

Although there have been many studies on effects of Fe_3O_4 nanoparticles in A549 cells [17, 18, 19, 20], to the best of our knowledge, there is no work related to the effects of Fe/Fe_3O_4 core-shell particles on these cells. Previous studies show concentration-dependent toxicity of Fe_3O_4 nanoparticles where a significant effect was observed only for concentrations of 100 µg/ml and higher [17, 18, 19]. Hence, particles are coated to reduce their potential toxic effects, so that they can be used with drugs in nanomedicine [18]. The toxicity of the magnetite nanoparticles is due to the increasing level of lipid peroxidation and decreasing antioxidant enzymes of human lung alveolar epithelial cells (A549), displaying a concentration-dependent toxicity in vitro [17]. Malvindi et. al. proposed that following the intake of nanoparticles by the cells, nanoparticles start to degrade and release Fe ions, which interact with hydrogen peroxide produced by the mitochondria. This process induces the generation of highly reactive hydroxyl radicals and ferric ions (Fe3+) through the Fenton reaction. Therefore, hydroxyl radicals and ferric ions could damage DNA, leading to cell death [18].

In our study, contradictory to the aforementioned previous studies, it has been found that the synthesized particles are toxic at such low concentrations down to 1 µg/ml. In order to evaluate the cytotoxicity level of NP1 on A549 cells, an additional cytotoxicity experiment with a common chemotherapeutic agent, Paclitaxel was performed on the same cell line. The IC50 value of this drug on A549 cells was found to be 11.1 µg/ml (Figure 7). This data shows that NP1 with an IC50 value of 1 µg/ml is more toxic on A549 cells in comparison to Paclitaxel.

We explain the high toxicity of the nanoparticles via Fenton reaction; following the degradation of Fe_3O_4, Fe core is exposed which accelerates the release of Fe ions and this leads to cell death. In order to further prove this hypothesis, particles with a thicker Fe_3O_4 shell was also synthesized (NP2). The IC50 values of this thicker shelled nanoparticles were 29 µg/ml and 27 µg/ml in NIH3T3 and A549 cells, respectively. The cell viability versus log concentrations are given in Figure 8. Surprisingly, no significant change was observed in NIH3T3 and A549 cell lines after treating them with thicker shelled nanoparticles in scratch assay (data not shown). As stated above, thicker Fe_3O_4 shell de-accelerates the degradation of the nanoparticles, consecutively slows down the cell death process.

Rosman et al. recently evaluated the effects of Gallic acid (GA) on A549 cells. IC50 values found for GA, Fe_3O_4-PEG-GA and Doxorubicin were 56 µg/ml, 13 µg/ml and 0.58 µg/ml, respectively [20]. Synthesized

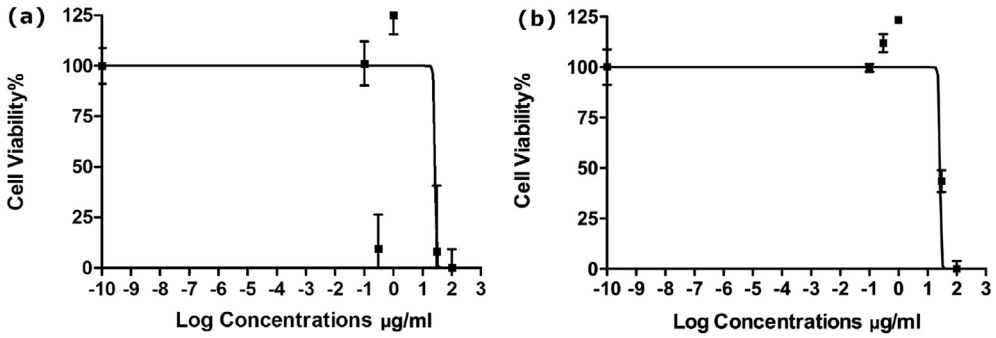

Figure 8. a. and b. Cell viability versus concentration plots of the nanoparticles NP2 at 0, 100 ng/ml, 300 ng/ml, 1 µg/ml, 3 µg/ml, 10 µg/ml, 30 µg/ml and100 µg/ml concentrations on NIH3T3 and A549 cells.

NP1 nanoparticles in this study have a lower IC50 value (1 μg/ml) in comparison to GA coated nanoparticles. This data supports the hypothesis that NP1 is a promising nanoparticle that can be used as a potential anti-cancer agent.

5. Conclusions

In summary, Fe/Fe_3O_4 core/shell nanoparticles with an average size of 20 nm and 13 nm have been synthesized and their performance has been evaluated in vitro. The effect of the nanoparticles on proliferation/survival and motility of NIH3T3 and A549 cells was assessed by cytotoxicity and scratch assays, respectively. IC50 value of NP1 was found to be 27.5 μg/ml in NIH3T3 and 1 μg/ml in A549 cells. This data indicates that the nanoparticles are more toxic to cancer cells. Comparatively, while the nanoparticles did not have any inhibitory effect on the motility of NIH3T3 cells, they showed a significant inhibitory effect on the motility of A549 lung cancer cells. The nanoparticles were found to be 100 times more toxic on cells when compared to the previous studies. This cellular phenomenon can be explained by the accelerated decomposition of particles due to the Fe core.

Declarations

Author contribution statement

B. H. Domac; Performed the experiments.

S. AlKhatib; Performed the experiments; Wrote the paper.

O. Zirhli; Performed the experiments.

N. G. Akdogan; Conceived and designed the experiments; Analyzed and interpreted the data.

Ş. C. Öçal Dirican; Performed the experiments.

G. Bulut; Conceived and designed the experiments; Analyzed and interpreted the data; Wrote the paper.

O. Akdogan: Conceived and designed the experiments; Analyzed and interpreted the data; Wrote the paper.

Funding statement

This work was supported by Bahçeşehir University's internal fund (BAP.2018–2.05).

Competing interest statement

The authors declare no conflict of interest.

Additional information

No additional information is available for this paper.

Acknowledgements

Authors would like to thank Dr. Gülcan Çorapcıoğlu (Sabancı University Nanotechnology Research and Application Center), and Prof. Dr. Ilker Küçük (Uludağ University) for TEM and VSM studies, respectively.

References

[1] M. Arruebo, N. Vilaboa, B. Sáez-Gutierrez, Assessment of the evolution of cancer treatment therapies, Cancers 3 (3) (2011) 3279–3330.

[2] L.S. Arias, J.P. Pessan, A.P.M. Vieira, T.M.T. Lima, A.C.B. Delbem, D.R. Monteiro, Iron oxide nanoparticles for biomedical applications: a perspective on synthesis, drugs, antimicrobial activity and toxicity, Antibiotics 7 (2) (2018) 46.

[3] H. Yang, Targeted nanosystems: advances in targeted dendrimers for cancer therapy, Nanomedicine 12 (2) (2015) 309–316.

[4] S.C. Baetke, T. Lammers, F. Kiessling, Applications of nanoparticles for diagnosis and therapy of cancer, Br. J. Radiol. 88 (1054) (2015) 20150207.

[5] Q. Zhou, L. Zhang, H. Wu, Nanomaterials for cancer therapies, Nanotechnol. Rev. 6 (5) (2017) 473–496.

[6] N. Schleich, et al., Comparison of active, passive and magnetic targeting tumors of multifunctional paclitaxel/SPIO-loaded nanoparticles for tumor imaging and therapy, J. Control. Release 194 (2014) 82–91.

[7] H. Maeda, Tumor-selective delivery of macromolecular drugs via the EPR effect: background and future prospects, Bioconjug. Chem. 21 (2010) 797–802.

[8] K. Greish, Enhanced permeability and retention (EPR) effect for anticancer nanomedicine drug targeting. Cancer Nanotechnology, Springer-Verlag, 2010, pp. 25–37.

[9] J. Chang, K. Chang, D. Hwang, Z. Kong, In vitro cytotoxicity of silica nanoparticles at high concentrations strongly depends on the metabolic activity type of the cell line, Environ. Sci. Technol. 41 (6) (2007) 2064–2068.

[10] R.K. Gilchrist, et al., Selective inductive heating of lymph nodes, Ann. Surg. 146 (1957) 596.

[11] U. Hafeli, W. Schutt, J. Teller, M. Zborowski, Scientific and Clinical Applications of Magnetic Carriers, Plenum Publishing Corporation, New York, 1997.

[12] J.S. Suk, Q. Xu, N. Kim, J. Hanes, L.M. Ensigna, PEGylation as a strategy for improving nanoparticle-based drug and gene delivery, Adv. Drug Deliv. Rev. 99 (Pt A) (2016) 28–51.

[13] F.H. Chen, L.M. Zhang, Q.T. Chen, Y. Zhang, Z.J. Zhang, Synthesis of a novel magnetic drug delivery system composed of doxorubicin-conjugated Fe_3O_4 nanoparticle cores and a PEG-functionalized porous silica shell, Chem. Commun. 46 (2010) 8633–8635.

[14] S.D. Li, L. Huang, Stealth nanoparticles: high density but sheddable PEG is a key for tumor targeting, J. Control. Release 145 (2010) 178–181.

[15] B. Kong, J. Seog, L. Graham, S. Lee, Experimental considerations on the cytotoxicity of nanoparticles, Nanomedicine 6 (5) (2011) 929–941.

[16] P. Orlowski, M. Zmigrodzka, E. Tomaszewska, Tannic acid-modified silver nanoparticles for wound healing: the importance of size, Int. J. Nanomed. 13 (2018) 991–1007.

[17] M. Watanabe, M. Yoneda, A. Morohashi, Y. Hori, D. Okamoto, A. Sato, D. Kurioka, T. Nittami, Y. Hirokawa, T. Shiraishi, K. Kawai, Effects of Fe_3O_4 magnetic nanoparticles on A549 cells, Int. J. Mol. Sci. 14 (2013) 15546–15560.

[18] M.A. Malvindi, V. De Matteis, A. Galeone, V. Brunetti, G.C. Anyfantis, Toxicity assessment of silica coated iron oxide nanoparticles and biocompatibility improvement by surface engineering, PLoS ONE 9 (1) (2014), e85835.

[19] S. Dwivedi, Synthesis, characterization and toxicological evaluation of iron oxide nanoparticles in human lung alveolar epithelial cells, Colloids Surfaces B Biointerfaces 122 (2014) 209–215.

[20] R. Rosman, B. Saifullah, S. Maniam, D. Dorniani, H. Mohd Zobir, F. Sharida, Improved anticancer effect of magnetite nanocomposite formulation of GALLIC acid (Fe_3O_4-PEG-GA) against lung, breast and colon cancer cells, Nanomaterials 8 (2018) 83.